



Isolation and investigation of the structure of silicon quantum dots from rice husk ultrafine silica for possible applications in nanoelectromechanical systems

K. M. Omatola^{a,*}, A. D. Onojah^b, R. Larayetani^c, A. O. Ohiani^a, I. I. Oshatuyi^a, M. B. Ochang^d, L. O. Anawo^a, P. Abraham^a

^aDepartment of Physics, Kogi State University, Anyigba, Nigeria

^bDepartment of Physics, Joseph Sarwuan Tarka University, Makurdi, Benue State, Nigeria

^cDepartment of Pure and Industrial Chemistry, Kogi State University, Anyigba, Nigeria

^dDepartment of Industrial Physics, Joseph Sarwuan Tarka University, Makurdi, Benue State, Nigeria

Abstract

Silicon quantum dots (SiQDs) are nanostructure semiconducting crystalline particles of silicon, usually less than 10 nm in size. Usually, silicon is extracted from its oxide through a carbothermic process using electric submerged arc furnaces at temperatures exceeding 2000 °C, a highly energy-intensive method and detrimental to silicon oxide's structural properties, resulting in carbon dioxide emissions. In this work, we propose a two-step green approach involving sol-gel synthesis and solid state magnesiothermic reduction at 700 °C to produce silicon quantum dots from rice husk ash. This method prevents strain, fracture, and vaporization associated with direct reduction methods at higher temperatures, which emit greenhouse gases and vaporize silicon. The produced silicon quantum dots were characterized using Energy Dispersive Spectroscopy (EDS), Transmission Electron Microscopy (TEM), and X-ray Diffraction (XRD) techniques. A total yield of 77.76% silicon, with average particle and crystallite sizes of 2.51 nm and 2.69 nm, respectively was observed. The material exhibited a dislocation density of 0.14 (14 %) lines/nm², strain of 0.0467 (4.67%), stress of 7.94 GPa, Young modulus of 170 GPa, and energy density of 32.50 GJm⁻³. These indicate robust mechanical properties that are suitable for nanoelectromechanical systems (NEMS) fabrication. In addition, this eco-friendly method used in this work utilizes rice husk silica which prevent the use of synthetic and harmful silica precursors. Thus, enhances sustainability and cost-effectiveness in accordance with green synthesis principles and the use of local resources.

DOI:10.46481/jnsps.2025.2690

Keywords: Silicon quantum dots, Rice husk silica, Sol-gel, Magnesiothermic reduction

Article History :

Received: 17 February 2025

Received in revised form: 02 August 2025

Accepted for publication: 21 August 2025

Available online: 23 September 2025

© 2025 The Author(s). Published by the Nigerian Society of Physical Sciences under the terms of the [Creative Commons Attribution 4.0 International license](https://creativecommons.org/licenses/by/4.0/). Further distribution of this work must maintain attribution to the author(s) and the published article's title, journal citation, and DOI.

Communicated by: C. A. Onate

1. Introduction

Silicon is the second most abundant element in the Earth's crust and ranks eighth in the universe. It occurs in nature predominantly in a combined state, mainly as oxides and silicates.

It is a brittle, hard, crystalline tetravalent metalloid whose particle size may vary when isolated. As a fundamental semiconductor material, it serves as the building block for several areas of electronic engineering, including telecommunications, sensing technologies, photonics, and lighting [1]. Among silicon-based nanomaterials, silicon quantum dots (SiQDs) have garnered significant researcher's interest due to their low toxicity, environmental friendliness, and potential applications in electron-

*Corresponding author Tel. No.: +234-813-133-5720.

Email address: komatola@yahoo.com (K. M. Omatola)

ics, mechanical system configurations and biomedical [2, 3]. In nanoelectromechanical systems (NEMS), silicon plays a dual role. It is used both as a substrate due to its compatibility with semiconductor fabrication processes and as a structural material in NEMS devices [4]. NEMS technologies often utilize elastic materials, selected based on parameters like Young's modulus, to fabricate multi-part joints and linkages [4]. Silicon-based nanomaterials have been effectively used to build resonant NEMS devices for applications such as ultrasensitive mass and force sensing, ultra-low-power RF signal generation, timing systems, and switching components [5].

Widely cited values of Young's modulus (E) for silicon range between 130–188 GPa, as determined by techniques such as quantum mechanical modeling and X-ray diffraction (XRD) [4]. In 1982, Peterson [6] reported a value of 190 GPa Young's modulus for silicon, which he used to calculate the resonant frequency of a silicon-based mirror device to be 16.3 kHz. The resonant frequency is crucial for evaluating a device's sensitivity to oscillation and its ability to withstand shock or vibration. Understanding the mechanical properties of materials is essential for evaluating their potential in various applications [7]. Such properties when accurately measured can provide useful information about the design and performance expectations of devices made from those materials [8].

Materials science and engineering integrate the study of processing, characterization, properties, and performance of materials. Failure and unreliability often stem from inadequate processing, impurities, or insufficient pre-application characterization. The increasing rate of failures in both mobile and static structures has raised serious concerns among NEMS developers. As a result, there is a growing emphasis on continuous structural assessment to ensure integrity and reliability. Notably, silicon's relative abundance, eco-friendliness, low operational potential, high surface area, robust mechanical features, and fast lithium/electron transport capacity make it a highly suitable material for enhancing energy and power densities in lithium-ion batteries [9, 10]. It has been reported that elastic modulus can be evaluated via compression tests and XRD techniques, particularly for fragile materials like silica-based aerogels [7]. In their work, the authors recommended XRD, a non-destructive method, for estimating the mechanical properties of nanomaterials. Traditional mechanical testing methods such as tensile, flexural, and indentation tests are often destructive, expensive, and unreliable at the nanoscale. Lin et al. [11] argued that XRD is a better alternative for assessing the mechanical features of semiconductors and related materials [12]. The technique is widely recognized for its ability to perform structural characterization, including phase identification, particle size estimation, crystallographic orientation, dislocation density, residual stress/strain measurement, and detection of phase transformations [12, 13]. For SiQDs, investigating mechanical properties such as dislocation density, strain, stress, and Young's modulus is critical for predicting the performance and reliability of future devices. Dislocation density measures the number of crystalline defects, which can affect mechanical strength and electrical performance, strain indicates the extent of elastic deformation before permanent change occurs, stress

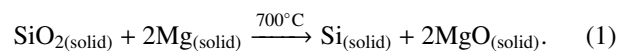
refers to internal forces developed within the material under external loads while Young's modulus quantifies material stiffness, i.e., resistance to deformation.

Historically, the isolation of elemental silicon from silica involved a carbothermic reduction process using electric arc furnaces at a temperature greater than 2000 °C, which consumes high energy and emits CO₂ as a greenhouse gas [14]. In contrast, recent studies have demonstrated magnesiothermic reduction of coastal sand-derived silica at lower temperatures (~800 °C) to isolate silicon nanoparticles while minimizing structural damage, strain, or vaporization [15]. In this study, we present a two-step green synthesis route for isolating silicon quantum dots from rice husk ash (RHA). Unlike the conventional single-step reduction methods which often involve environmentally harmful processes, this method employs a sol-gel synthesis followed by thermochemical treatment. Characterization techniques such as energy dispersive spectroscopy (EDS), transmission electron microscopy (TEM), selected area electron diffraction (SAED), and XRD were employed to analyze purity, particle size, and crystalline phase of SiQDs. The results indicate a high-purity, polycrystalline structure with nanometric dimensions, confirming the formation of SiQDs. These SiQDs exhibit robust mechanical characteristics, making them highly suitable for NEMS fabrication. Furthermore, this green synthesis approach introduces a novel and eco-friendly method for producing quantum-grade silicon from abundant agricultural waste, offering significant economic and environmental advantages.

2. Experimental details

2.1. Solid state isolation of SiQDs

The sol – gel technique employed is previously describe in [12] to obtain the ultrafine rice husk silica of high purity, low dislocation density, and minimal associated lattice strain. The magnesiothermic reduction is a solid-state synthetic technique involving the reaction of the high purity silica aerogel from the green source (rice husk) and magnesium powder, mixed in ratio 1:2 in a platinum crucible and heated at 700 °C in a muffle furnace for half an hour according to the stoichiometric as shown in Eq. (1):



2.2. Characterizations of SiQDs

The as obtained SiQDs was collected, stored in airtight bottle for EDS, XRD and TEM analyses at Rolab Diagnostic Laboratory, Ibadan, Nigeria. The EDS machine of model JEOL JSM-7600F is use to analyze the elemental composition (the quantity as well quality of silicon quantum dots and associated elements) and morphology of the produced SiQDs, respectively. The investigation of the shape, particle sizes and SAED pattern are done with the use of JEM-ARM200F-G model of a transmission electron microscope. TEM image gives the particle sizes and shapes whereas SAED pattern signifies the crystallinity of the SiQDs. The X-ray diffraction studies of

the SiQDs were done using PW X-ray diffractometer (Rigaku D/Max-III C model) with the following specifications: a CuK α radiation ($\lambda = 0.1541$ nm), step size of 0.020 at a scanning range of 20° - 60° at 2θ angle ; a voltage of 45 kV, a current of 20 mA. The data obtained are use to estimate the crystallite size, dislocation density, lattice strain, Young modulus, stress, energy density. These represent mechanical properties, and deduction of the phase constitution.

2.2.1. Elemental analysis via energy dispersive X-ray spectroscopy (EDS)

EDS is a non-destructive quantitative analytical technique for the identification of the elemental composition of materials when excited by electron beam causing them to emit radiation detectable by an EDS detector which converts the rays into electrical pulses or spectrum to be analyzed for specific elements. This is essential and foremost in materials characterizations since it reveals the constituents of the produced material.

2.2.2. Transmission electron microscopy (TEM)

TEM employs a beam of electrons to make available a highly resolved image (morphology) of a material under examination. The range of particle diameters (sizes) is estimated from the TEM image. The average value, t of sizes of the TEM images is computed by summing the various sizes and dividing by the number of shapes present. The value obtained is used to infer that the produced materials are quantum dots with varying sizes and shapes. Selected area electron diffraction (SAED) pattern depicts the phase of the produced material. It is a complimentary structural characterization technique to TEM image in term of dislocation in a material using the presence or absence of streaks [13].

2.2.3. Crystallite size

The Scherrer equation depicted in Eq. (2) [15] is used to estimate the crystallite size, D :

$$D = \frac{0.9\lambda}{\beta \cos \theta}, \quad (2)$$

where λ denotes wavelength, β is full width at half maximum and θ is diffracting angle. The determination of the crystallite size is done from the X-ray diffraction profile analyses for the intensity against 2θ plots of the investigated SiQDs.

2.2.4. Dislocation density

The dislocation density, δ is a measure of irregularity in a crystal due to the growth accident or drying process. It connotes the number of dislocation lines per unit volume of crystal whose value illustrates the degree of crystallinity of the SiQDs profiles [16] and is calculated from Eq. (3):

$$\delta = \frac{1}{D^2}. \quad (3)$$

2.2.5. Elastic strain

The strain value indicates the extent to which the material can deform elastically before undergoing permanent deformation and its value was calculated from Eq. (4). It is associated with structural defects or imperfection such as grain boundary and increases with increasing crystallite size [17, 18].

$$\text{Elastic strain, } \varepsilon = \frac{\beta}{4 \tan \theta}. \quad (4)$$

2.2.6. Young's modulus

The Young's modulus measures the stiffness of the produced SiQDs, that is, how much it resists deformation under stress. It is defined as:

$$\text{Young modulus, } E_{(hkl)} = \frac{\sigma}{\varepsilon}, \quad (5)$$

where

$$\frac{1}{E_{(hkl)}} = \frac{S_{11} - 2S_{12}[(hk)^2 + (hl)^2 + (kl)^2]}{[h^2 + k^2 + l^2]}, \quad (6)$$

hkl represents Miller indices or directional plane, σ represents stress, and ε represents elastic strain.

Heryanto *et al.* [19] defined S as compliance whose value for silicon, are $S_{11} = 7.68 \times 10^{-12}$ m²/N and $S_{12} = 3.54 \times 10^{-12}$ m²/N. Theoretically,

$$E_{(\text{QDs})} = \frac{E_{(\text{bulk})}}{1 + \frac{\beta}{t}}, \quad (7)$$

where $E_{(\text{QDs})}$ is elastic modulus of silicon quantum dots, $E_{(\text{bulk})}$ is elastic modulus of bulk silicon, approx. 190 GPa, β is a constant dependent on the material and size range (typically around 1 – 10 nm), and t is diameter of the quantum dot.

2.2.7. Stress

Stress value as another mechanical parameter represents the internal forces per unit area within the SiQDs when subjected to external forces. It is estimated using:

$$\text{Stress, } \sigma = E\varepsilon. \quad (8)$$

2.2.8. Energy density

The energy density of a material describes the per unit volume of energy storage. It is a desirable quantity of interest in batteries, supercapacitors, and optoelectronics applications. Its value can be estimated using Eq. (9). The energy density for the SiQDs crystal is given by [20]:

$$U = \frac{\varepsilon^2 E_{(hkl)}}{2}. \quad (9)$$

3. Results and discussion

Figure 1 depicts the EDS analysis spectrum of the rice husk ultrafine silica (SiO₂). It was observed that Si is the most prominent element with concentration of 64.2 % by weight and other trace elements, like calcium (Ca), iron (Fe), oxygen (O), carbon (C), magnesium (Mg), and gold (Au) have a total concentration

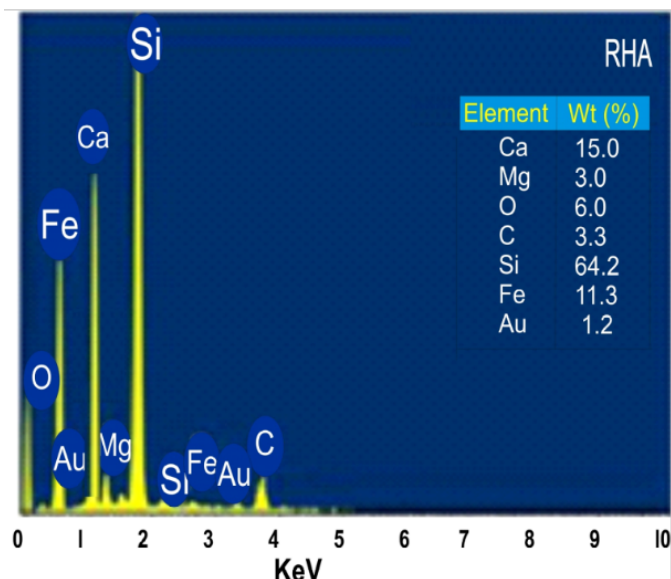


Figure 1: Elemental composition of the rice husk aerogel (RHA) ultrafine silica from EDS analysis showing silicon as the prominent element.

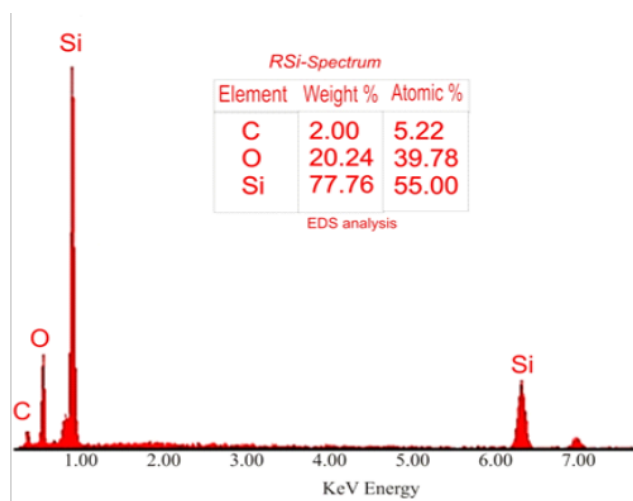


Figure 2: Elemental composition through EDS of silicon quantum dots obtained from the reduced rice husk aerogel (RHA) ultrafine silica by magnesiothermic process.

of 35.8 % by weight. This relatively high concentration of Si compared to available record is quite encouraging to isolate silicon for further purification.

Figure 2 shows the EDS spectrum of rice husk ultrafine silica after the thermochemical reduction process. The spectrum shows Si with percentage concentration of 77.76 % S while the remaining percentage consists of carbon and oxygen. The thermochemical reduction process for the isolation of Si has eliminated Ca, Fe, Mg, and Au earlier found in the rice husk ultrafine silica (RHA) as depicted in Figure 1 which serves as a bulk material. The result reveals a high yield of Si because of the removal of oxygen during the reduction reaction of SiO_2 by the magnesium element. In addition, the reduced carbon con-

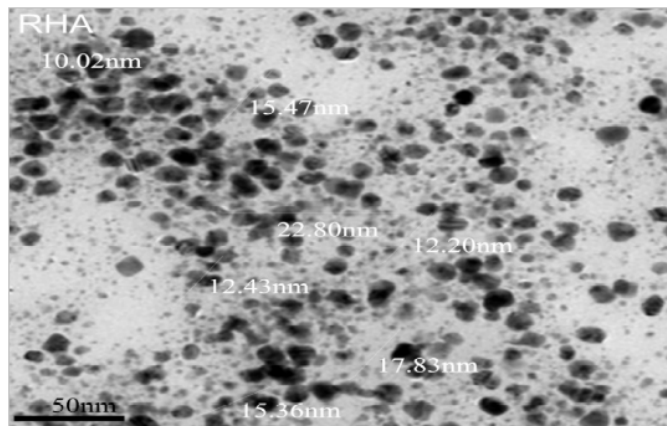


Figure 3: TEM image of the rice husk aerogel (RHA) ultrafine silica as the bulk material Ref. [13].

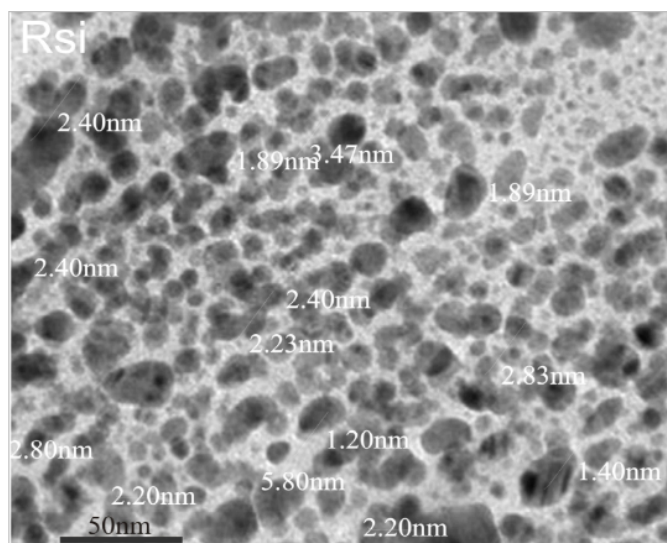


Figure 4: TEM image of the silicon quantum dots (RSi) derived from the reduced rice husk aerogel ultrafine silica.

centration is due to its burn out during the thermochemical reaction, and the increased oxygen concentration arises from contamination with the environment (air and machine). The high purity of the produced silicon quantum dots without heavy metals like cadmium, indium, lead and other contaminants reveal their biocompatibility and non-toxic structures.

The morphology of the SiO_2 used as the bulk material is shown in Figure 3. The image obtained from the transmission electron microscope at a scale bar of 50 nm reveals a disperse irregular oval shapes with particles sizes ranging from 10.02 - 22.80 nm and mean value of 15.12 nm, which indicate the dimension of an ultrafine (nano) material. These irregular and multi-dimensional oval shapes enhance surface area, mechanical strength, catalytic properties, optical performance, and utilization in biomedical applications [13].

Figure 4 is the image from the transmission electron microscopy of the silicon quantum dots obtained from the reduced SiO_2 . The particle size ranges from 1.20 - 5.80 nm while the av-

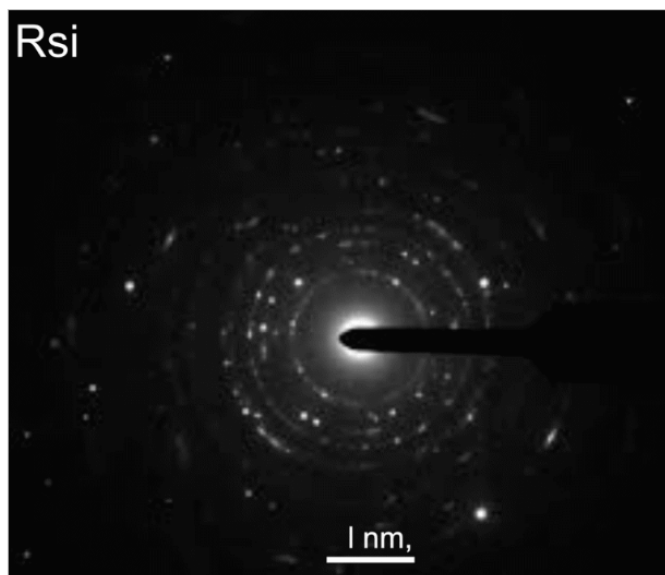


Figure 5: SAED pattern of the silicon quantum dots showing bright spots in ring form, an affirmation of the polycrystallinity of the quantum material.

erage value particle size is 2.51 nm, which is about one-third of the bulk material's size. This suggests that the produced silicon quantum dots are in the strong quantum confinement domain and are less than the exciton Bohr radius of silicon demonstrating a potential application in optoelectronics and biomedical fields [2]. The particle distribution shows varying elongated oval shapes with little agglomeration in contrast to the bulk SiO_2 shown in Figure 3. This suggests improved optical and electronic properties that is useful in bio - imaging and optoelectronic devices.

Figure 5 depicts the SAED pattern for the SiQDs which shows bright spots and rings. This confirms the crystalline nature and the randomly dotted spots in ring form confirms the polycrystalline nature of the SiQDs [22]. The concentric rings and diffraction spots are consistent with a material that has multiple orientations of its crystallographic planes. The concentric rings indicate the polycrystalline nature of the sample, and the bright spots correspond to diffraction from specific crystallographic planes which in real sense also compliments the result of the XRD spectrum [13].

Figure 6 provides the X-ray diffraction (XRD) spectrum of the produced SiQDs material labeled "RSi." The XRD pattern identifies several peaks corresponding to the crystallinity of the material and an exceptional peak for MgO. The spectrum comprises primarily a quartz phase pronounced on the following direction of planes at 2θ angles: (100, 20.8°), (101, 26.6°), (110, 36.6°), (201, 46.6°), (112, 50.1°), (211, 60.0°). The peak intensity occurs at 5000 units along the vertical axis corresponding to 26.6° 2-theta along the horizontal direction, an indicative of where most of the atoms of the produced SiQDs material is concentrated. However, a minor peak at around 38.9° 2-theta on (102) direction corresponds to magnesium oxide, MgO impurity that could be attributed to incomplete separation during

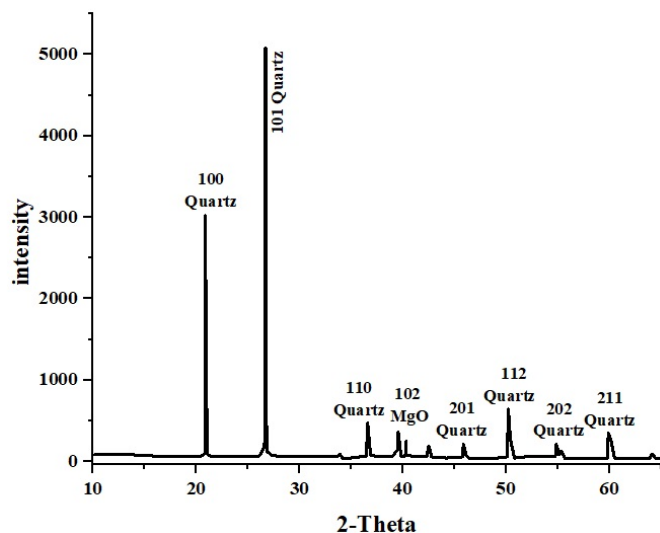


Figure 6: XRD spectrum of silicon quantum dots (SiQDs) showing phase constitution and miller indices.

preparation [23].

The Figure 6 further illustrates all the detectable peaks with their respective hkl values for the investigated SiQDs. All the detectable peaks are indexed as face centre cubic (FCC) structure found in the standard reference data for Si: JCPDS 03–0544 [24]. The crystal structure is face centre cubic (FCC) as all the (h,k,l) is odd and their sum not all even [12].

The details derivable from the XRD spectrum are used to investigate the crystallite size, dislocation density, strain, stress, Young's modulus, and energy density associated with the structure of the isolated SiQDs, hence the prediction of the mechanical properties of the produced material.

The crystallite size, D obtained from Eq. (2), ranges from 1.13 nm to 3.89 nm with a computed average or mean value of 2.69 nm signifying a relatively small crystallite core consistent with quantum dots materials. Furthermore, the overall particle size obtained from TEM is slightly smaller than the crystallite size and both values approximate to the Bohr radius of silicon (2.20 - 2.50 nm). This result highlights the possible strong exhibition of quantum confinement, enhance surface area, and tunable optical effects suitable in biosensing, catalysis and optoelectronics applications [2].

The average dislocation density which is the measure of the overall defects or imperfections associated with the SiQDs is calculated using equation (3) to be 0.14 (or 14 %) lines per square nm. This shows that the SiQDs are relatively defect-free crystalline structure connoting 86 % streak free structure. This low dislocation is corroborated in the SAED pattern obtained for the SiQDs as there exist no streaks in the structure [13]. This finding is crucial for electronic applications, as the produced material shows minute dislocations that can act as charge traps and recombination centers which could have reduced the performance and efficiency of devices based on the synthesized dots.

The average elastic strain value of 4.67 % was obtained

from Eq. (4) indicating the extent to which the produced SiQDs material can deform elastically before undergoing permanent deformation. The value of 4.67 % suggests that the SiQDs can withstand a moderate level of deformation, which is beneficial for applications requiring flexibility and resilience, such as flexible electronics and sensors. Young's modulus is an important mechanical parameter which expresses the stiffness of the SiQDs i.e. how much it can resist deformation under stress. The average Young's modulus of 170 GPa obtained from Eq. (5) is relatively high, implying that the SiQDs are quite stiff and will maintain their shape under significant mechanical forces. This property is essential for maintaining structural integrity in high-precision applications such as optical and electronic devices.

Another mechanical property of high interest computed from Eq. (8) represents the internal forces per unit area within the SiQDs when subjected to external forces. The average value of 7.94 GPa computed reveals that the SiQDs material can endure high mechanical forces before yielding or breaking. This high stress tolerance is advantageous for applications in nanoelectromechanical systems (NEMS) and other devices where mechanical robustness is critical.

The calculated value of an average of 32.5 GJ/m³ was obtained from Eq. (9). The value signifies a possibility of high energy storage per unit space, suggesting the suitability of the produced silicon quantum dots for compact as well efficient energy storage.

4. Conclusion

The lower temperature isolation of the SiQDs from the prepared ultrafine silica of plant origin has shown a high yield, purity, and robust structural properties suitable for a wide range of applications especially in nanoelectronics and mechanical systems. The successful extraction and isolation of the produced quantum dots material supports an eco-friendly approach advancing the promotion of sustainable and cost effectiveness aligned with green chemistry principles and local content initiative.

Data availability

The data will be available on request from the corresponding author.

References

- [1] S. Ghosh, S. Saha & D. Das, "Silicon: a critical review on its role in modern electronic and photonic devices", *Materials Today: Proceedings* **18** (2019) 4326. <https://doi.org/10.1016/j.matpr.2019.07.404>.
- [2] S. Morozova, M. Alikina, A. Vinogradov & M. Pagliaro, "Silicon quantum dots: Synthesis, encapsulation, and application in light-emitting diodes", *Frontiers in Chemistry* **8** (2020) 191. <https://doi.org/10.3389/fchem.2020.00191>.
- [3] D. Beri, "Silicon quantum dots: Surface matter, what next?", *Materials Advance* **4** (2023) 3380. <https://doi.org/10.1039/d2ma0984f>.
- [4] M. A. Hopcroft & D. N. William, "What is the Young's modulus of silicon?", *Journal of micromechanical systems* **19** (2010) 229. <https://doi.org/10.1109/JMEMS.2009.2039695>.
- [5] H. Yu, W. W. Zhang, S. Y. Lei, L. B. Lu, C. Sun & Q. A. Huang, "Study on vibration behavior of doubly clamped silicon nanowires by molecular dynamics", *Journal of Nanomaterials* **2012** (2012) 342329. <https://doi.org/10.1155/2012/342329>.
- [6] K. Petersen, "Silicon as a mechanical material", *Proceedings of the IEEE* **70** (1982) 420. <https://doi.org/10.1109/PROC.1982.12331>.
- [7] C. Bi, G. H. Tang, C. B. He, X. Yang & Y. Lu, "Elastic modulus prediction based on thermal conductivity for silica aerogels and fiber reinforced composites", *Ceramics International* **48** (2022) 6691. <https://doi.org/10.1016/j.ceramint.2021.11.219>.
- [8] K. M. Omatola & A. D. Onojah, "Elemental analysis of rice husk ash using X-ray fluorescence technique", *International Journal of Physical Sciences* **4** (2009) 189. <https://doi.org/10.5897/IJPS.9000217>.
- [9] X. Su, Q. Wu, J. Li, X. Xiao, A. Lott, W. Lu, W. Brian, W. Sheldon & J. Wu, "Silicon-based nanomaterials for lithium-ion batteries: A Review", *Advanced Energy Materials* **4** (2014) 1300882. <https://doi.org/10.1002/aenm.201300882>.
- [10] J. Entwistle, A. Rennie & S. Patwardhan, "A review of magnesiothermic reduction of silica to porous silicon for lithium-ion battery applications and beyond", *Journal of Materials Chemistry A* **6** (2018) 18344. <https://doi.org/10.1039/C8TA06370B>.
- [11] K. Lin, Y. Yu, J. Xi, H. Li, Q. Guo, J. Tong, & L. Su, "A fibre-coupled self-mixing Laser diode for the measurement of Young's modulus", *Sensors* **16** (2016) 928. <https://doi.org/10.3390/s16060928>.
- [12] A. Ali, Y. W. Chiang & R. M. Santos, "X-ray diffraction techniques for mineral characterization: A review for engineers of the fundamentals, applications and research directions", *Minerals* **12** (2022) 1. <https://doi.org/10.3390/min12020205>.
- [13] K. M. Omatola, A. D. Onojah, A. N. Amah & I. Ahemen, "Synthesis and characterization of silica xerogel and aerogel from rice husk ash and pulverized beach sand via sol-gel route", *Journal of the Nigerian Society of Physical Sciences* **5** (2023) 1609. <https://doi.org/10.46481/jnps.2023.5.1609>.
- [14] Y. Sakaguchi, M. Ishizaki, T. Kawahara, M. Fukai, M. Yoshiyagawa & F. Aratani, "Production of high purity silicon by carbothermic reduction of silica using AC-arc furnace with heated shaft", *ISIJ International* **32** (1992) 643. <https://doi.org/10.2355/isijinternational.32.643>.
- [15] S. S. Oluyamo, O. F. Famutimi & M. O. Olosoji, "Isolation and characterization of high grade nanosilicon from coastal landform in Ilaje local government area of Ondo state, Nigeria", *African Scientific Reports* **2** (2023) 82. <https://doi.org/10.46481/asr.2023.2.1.82>.
- [16] H. Sajid, K. S. Rakesh, S. K. Nishant & K. Gaurav, "Synthesis and characterization of crystalline nano silica from rice husk (agricultural waste) and its magnetic composites", *Research Square*, 2022. [Online]. <https://doi.org/10.21203/rs.3.rs-1785138/v1>.
- [17] I. W. Sutapa, A. W. Wahab, P. Taba & N. L. Nafie, "Dislocation, crystallite size distribution and lattice strain of magnesium oxide nanoparticles", *Journal of Physics Conference Series* **979** (2018) 1. <https://doi.org/10.1088/1742-6596/979/1/012021>.
- [18] S. Sarka, S. D. Ramarao, T. Das, R. Das, C. P. Vinod, S. Chakraborty & S. C. Peter, "Unveiling the roles of lattice strain and descriptor species on Pt-like oxygen reduction activity in Pd-Bi catalysts", *American Chemical Society Publications* **11** (2021) 800. <https://doi.org/10.1021/acscatal.0c03415>.
- [19] D. Kumar, M. Singh and A. K. Singh, "Crystallite size effect on lattice strain and crystal structure of $B_{1/4}Sr_{3/4}MnO_3$ layered Perovskite Manganite", *American Institute of Physics CP* **1953** (2018) 030185. <https://doi.org/10.1063/1.5032520>.
- [20] Heryanto, B. Abdullah, D. Tahir & Mahdalia, "Quantitative analysis of X-ray diffraction spectra for determine structural properties and deformation energy of Al, Cu and Si", *Journal of Physics, Conference series* **1317** (2018) 012052. <https://doi.org/10.1088/1742-6596/1317/1/012052>.
- [21] A. J. Suhir & H. H. Khalid, "A comprehensive study of Williamson-Hall method and size-strain method through x-ray diffraction pattern of cadmium oxide nanoparticles", *AIP conference proceedings* **2307** (2020) 020015. <https://doi.org/10.1063/5.0033762>.
- [22] C. F. Holder & R. E. Schaak, "Tutorial on powder x-ray diffraction for characterizing nanoscale materials", *American Chemical Society Nano* **13** (2019) 7359. <https://doi.org/10.1021/acsnano.9b05157>.

- [23] U. Kalapathy, A. Proctor, & J. Shult, "An improved method for production of silica from rice husk ash", *Bioresource Technology* **85** (2002) 285. [https://doi.org/10.1016/S0960-8524\(02\)00116-5](https://doi.org/10.1016/S0960-8524(02)00116-5).
- [24] S. K. Mishra, H. Roy, A. K. Lohar, S. K. Samanta, S. Tiwari & K. Dutta, "A comparative assessment of crystallite size and lattice strain in differently cast A356 aluminium alloy", *IOP Conference Series, Materials Science and Engineering* **75** (2015) 1. <https://doi.org/10.1088/1757-899X/75/1/012001>.